

## Electronic Supplementary Information (ESI)

### Synergetic Effect of Pyrrolic-N and Doped Boron in Mesoporous Carbon for Electrocatalytic Ozone production

Qiaoqiao Zhang,<sup>+</sup> Yongyong Cao,<sup>+</sup> Yilong Yan, Bowen Yuan, Haiyang Zheng, Yu Gu,  
Xing Zhong\* and Jianguo Wang\*

#### Table of Contents

1. Experimental Procedures .....	1
1.1 Chemicals and materials .....	1
1.2 Sample preparation .....	1
1.3 Characterization .....	1
1.4 Electrode preparation .....	2
1.5. Electrochemical ozone production measurements .....	2
1.6. O <sub>3</sub> concentration analysis .....	2
1.6.1 Qualitative analysis for the concentration of dissolved O <sub>3</sub> .....	2
1.6.2 Quantitative analysis for the concentration of dissolved O <sub>3</sub> .....	2
1.6.3 Qualitative analysis for the concentration of gaseous O <sub>3</sub> .....	3
1.6.4 Quantitative analysis for the concentration of gaseous O <sub>3</sub> .....	3
1.7. Calculation Section .....	4
2. Results and Discussion .....	5
3. References .....	37

## **1. Experimental Procedures**

### **1.1 Chemicals and materials**

F127 (BR, Sigma-Aldrich (Shanghai) Trading Co., Ltd), H<sub>3</sub>BO<sub>3</sub> (99.99 %, Aladdin Industrial Co., Ltd), Urea (≥99.5 %, Aladdin Industrial Co., Ltd), Ethanol (≥99.7 %, Sinopharm Chemical Reagent Co., Ltd), HNO<sub>3</sub> (AR, 65-68 %, Sinopharm Chemical Reagent Co., Ltd), Propanone (AR, ≥99.5 %, Sinopharm Chemical Reagent Co., Ltd), H<sub>3</sub>PO<sub>4</sub> (AR, ≥85.0 %, Sinopharm Chemical Reagent Co., Ltd), NaH<sub>2</sub>PO<sub>2</sub> (AR, 99.0 % Aladdin Industrial Co., Ltd), Na<sub>2</sub>S<sub>2</sub>O<sub>3</sub> (AR, ≥99.0 %, Sinopharm Chemical Reagent Co., Ltd), I<sub>2</sub> (AR, 99.0.8 % Aladdin Industrial Co., Ltd), Starch, Soloule (AR, ≥99.5 %, Sinopharm Chemical Reagent Co., Ltd), Indigotindisulfonate Sodium (96 % Aladdin Industrial Co., Ltd), Nafion PFSA Polymer (5.0-5.4 wt %, Suzhou Yilongcheng Energy Technology Co., Ltd.), Resol (self-made)<sup>1, 2</sup>, Carbon Fiber (CF, CeTech Co., Ltd), K<sub>2</sub>SO<sub>4</sub> (99 %, Aladdin Industrial Co., Ltd), Starch Iodide Paper (Shanghai Sanaisi Reagent Co., Ltd.), DPD Ozone Detection Kit (Hangzhou Lohand Biological Technology Co., Ltd.), Millipore deionized water was used to prepare all the solutions.

### **1.2 Sample preparation**

The D-BNC sample was obtained based on two-step polymerization and pyrolysis procedures. Briefly, a homogeneous mixture of boric acid and urea were used as the boron and nitrogen sources, respectively. Resol was used as a carbon precursor, and F127 as a pore-directing agent. To synthesize D-BNC, an aqueous solution containing resol (3.0 g), ethanol (4.0 g), F127 (0.5 g), boric acid (0–0.25 g) and urea (0–0.25 g) were mixed and sonicated for 15 min in an ultrasonic cell crusher noise isolating chamber at room temperature. Successively, this homogeneous precursor alcoholic solution was evaporated at room temperature and then, cured at 150 °C for 24 h with a heating rate of 5 °C/min. The dry precursor was heated to 350 °C in N<sub>2</sub> atmosphere for 180 min with a heating rate of 1 °C/min and then, carbonized at 900 °C for 120 min with a heating rate of 5 °C/min. Subsequently, the sample was ground into a powder thinner than 180 mesh by using a ball mill. The compound was then washed with deionized water at 80 °C to remove the oxide of boron and finally dried in a vacuum oven at 80 °C. The final products were labelled as D-BNC-x-y, where x defines the B:N ratio and y is the calcination temperature (800, 900, or 1000 °C). For the sake of simplicity, we refer to the D-BNC-1.5-900 as D-BNC in the manuscript. Moreover, when no urea, no boric acid, neither urea nor boric, and no F127, the samples are labelled as D-BC, D-NC D-C, and BNC, respectively. Simultaneously, some other comparative catalysts were also prepared. Such as the D-BNC with no holding pyrolysis time at 900 °C (D-BNC-1.5-900-A) or with 240 min holding pyrolysis time at 900 °C (D-BNC-1.5-900-B) were prepared. In addition, the D-BNC was prepared in Ar atmosphere is labelled as D-BNC-1.5-900-Ar.

### **1.3 Characterization**

Transmission electron microscopy (TEM) image was obtained by using Tecnaig<sup>2</sup>F30S-Twin at an acceleration voltage of 300 kV. The pore structure characteristics of the samples were determined by N<sub>2</sub> adsorption at –196 °C using Micromeritics ASAP2020HD88 volumetric sorption analyzer. BET surface area was calculated from the isotherm using the Brunauer–Emmett–Teller equation. Pore size distribution was calculated based on nonlocal density functional theory method on the basis of the adsorption branch. X-ray photoelectron spectroscopic (XPS) measurements were performed on ESCALAB 250Xi. The crystal structures of the samples were mainly characterized by X-ray diffraction (XRD) using X'Pert PRO. The Raman spectra were collected on Raman spectrometer (Renishaw) using in via Raman microscope. Elemental analysis (EA) measurements were performed on Elementar Vario

El cube. The Inductively Coupled Plasma Mass Spectrometry were collected on Agilent 720/730 Series ICP-OES.

### **1.4 Electrode preparation**

A carbon fiber (CF) was cut into slices (2 cm × 2 cm) and ultrasonicated in HNO<sub>3</sub> (40 wt %), acetone, ethanol, and deionized water for 30 min successively. The CF was then thoroughly washed initially with ethanol and successively with water. The sample was dried at 60 °C for further use. Several catalyst (4 mg) suspensions in ethanol (900 μL) were prepared by introducing 100 μL of Nafion solution as a binder while sonicating at 700 W for 30 min. To obtain the electrodes, a quantity of 1 mL of catalyst suspension was dropped onto the CF (1 mg/cm<sup>2</sup>) surface and then dried under infrared light.

### **1.5. Electrochemical ozone production measurements**

A series of electrochemical ozone production measurements was performed by using an electrochemical workstation (CHI760E) with a typical three-electrode cell. The D-BNC/CF sample was employed as the working electrode, a platinum wire was used as the counter electrode, and an Ag/AgCl electrode as the reference electrode. The activity of the electrocatalysts was measured twice via cyclic voltammetry (CV) and three times successively via linear sweep voltammetry (LSV). These electrochemical measurements were carried out in a saturated K<sub>2</sub>SO<sub>4</sub> solution at room temperature and the potentials were referred to the reversible hydrogen electrode (RHE) by using the Nernst equation:

$$E(RHE) = E(Ag/AgCl) + 0.194 V + 0.0592 \times pH$$

The stability of the electrocatalysts was evaluated via CV and by measuring the current versus time (IT) techniques for 100 h under 20 mA cm<sup>-2</sup>. The electrochemical measurements were carried out in a saturated K<sub>2</sub>SO<sub>4</sub> solution at room temperature.

### **1.6. O<sub>3</sub> concentration analysis**

#### **1.6.1 Qualitative analysis for the concentration of dissolved O<sub>3</sub>**

A series of electrochemical measurements was performed by using an electrochemical workstation (CHI760E) with a typical three-electrode cell. D-BNC/CF (β-PbO<sub>2</sub>/CF, D-BN/CF, D-NC/CF, D-C/CF, or CF) was employed as the working electrode, a platinum wire was used as the counter electrode, and the Ag/AgCl electrode as the reference one. A saturated K<sub>2</sub>SO<sub>4</sub> aqueous solution was used as the electrolyte. The activity of the electrocatalysts was evaluated via CV and IT for 10 min and at room temperature. A quantity of 100 mg O<sub>3</sub> water test powder was added into a 5 mL of electrolyte after the reaction and the color change of the solution for about 1 min. The results show that the darker the color is, the higher is the ozone water concentration.

#### **1.6.2 Quantitative analysis for the concentration of dissolved O<sub>3</sub>**

Indigo disulphonate spectrophotometry (IDS) was used to provide a quantitative analysis of the O<sub>3</sub> water concentration<sup>3</sup>. A quantity of 10 mL of a buffer solution with pH = 2.0, consisting of a mixture of phosphoric acid and sodium hypophosphite, was added to 0.75 mL of a 1 mM indigo

carmine solution into a 25 mL volumetric flask. In addition, an electrolyte was added after the EOP reaction has occurred to level the volume of the solution to the tick mark. The compound was mixed thoroughly. Finally, the absorbance of such solution at 610 nm was measured by using a SP-752PC UV-VIS spectrophotometer, and the O<sub>3</sub> water concentration was determined based on a standard curve (Fig. S16).

#### Standard curve of dissolved O<sub>3</sub> concentration

A quantity of 100 mL of pure water was flushed with gaseous O<sub>3</sub> for about 30 min and its pH was adjusted to < 3 by adding 0.5 mmol/L of H<sub>2</sub>SO<sub>4</sub>. The concentration of the solution was measured on a 25 mL sample by using the following procedure: adding 100 mL KI solution with 2 g KI, titrate with 0.05 mmol/L Na<sub>2</sub>S<sub>2</sub>O<sub>3</sub>, add a starch indicator to make the solution blue until the color turned pale yellow, and continue titration with 0.05 mmol/L Na<sub>2</sub>S<sub>2</sub>O<sub>3</sub> until the solution faded, record the amount of 0.05 mmol/L Na<sub>2</sub>S<sub>2</sub>O<sub>3</sub>.

$$C_{O_3} = V_{Na_2S_2O_3} * C_{Na_2S_2O_3} * \frac{2400}{V_{O_3}}$$

$V_{Na_2S_2O_3}$ : the amount of Na<sub>2</sub>S<sub>2</sub>O<sub>3</sub>

$C_{Na_2S_2O_3}$ : the concentration of Na<sub>2</sub>S<sub>2</sub>O<sub>3</sub>

$V_{O_3}$ : the amount of O<sub>3</sub>

The maximum absorbance of the indigo carmine solution detected with a SP-752PC UV-VIS Spectrophotometer measured 610 nm. A quantity of 10 mL of a buffer solution with pH = 2.0, consisting of a mixture of phosphoric acid and sodium hypophosphite, and 0.75 mL of a 1 mM indigo carmine solution, were added into 0, 2, 4, 6, and 8 mL of O<sub>3</sub> water. After the reaction the electrolyte solution was added to obtain a 25 mL volume and mixed for 1 min. Finally, the absorbance of the solution at 610 nm was measured by using a SP-752PC UV-VIS Spectrophotometer. The concentration gradient of the compound was calculated based on a standard curve.

#### **1.6.3 Qualitative analysis for the concentration of gaseous O<sub>3</sub>**

In order to provide a qualitative comparison the concentration of gaseous O<sub>3</sub> a series of electrochemical measurements was performed by using a galvanostat. A D-BNC/CF sample was used as the working electrode, a platinum sheet was employed as the counter electrode, and a saturated K<sub>2</sub>SO<sub>4</sub> aqueous solution as the electrolyte. A moistened starch potassium iodide test paper was suspended above the working electrode, in the anode, and operated constantly with different current values (6.25, 12.50, 18.75, 25.00, 31.25, and 37.50 mA cm<sup>-2</sup>). The color of the test paper was assessed for each currents leve<sup>4</sup>. Moreover, the galvanostat was operated at 100 mA for 2.5, 5.0, 7.5, 10.0, and 15.0 min, to compare the variations of the color of the test paper.

#### **1.6.4 Quantitative analysis for the concentration of gaseous O<sub>3</sub>**

A series of electrochemical measurements was performed by using a galvanostat, which was operated at 25 mA cm<sup>-2</sup>. A D-BNC/CF (β-PbO<sub>2</sub>/CF or CF) sample was used as the working electrode, a

platinum wire was employed as the counter electrode, and a saturated  $K_2SO_4$  aqueous solution as the electrolyte. Moreover, a sealed H-type electrolyzer was used as the electrolytic cell, which was connected to an ozone monitor (2B tech model 202 ozone monitor). All the experiments were conducted at room temperature.

### **1.7. Calculation Section**

DFT calculations were performed using the Vienna ab initio simulation package (VASP). The interactions between the ionic cores and valence electrons were described using a projector-augmented wave (PAW) method together with the generalized gradient approximation (GGA) and parameterized by Perdew-Burke-Ernzerhof (PBE) density functional. A plane wave cutoff energy was set to 450.0 eV. Charge transfer were calculated in terms of the Bader charge. DFT-D3 method was adopted for the Van der Waals correction. The Brillouin zone was sampled with a Monkhorst-Pack mesh of special k-points, together with  $5 \times 5 \times 1$  grid sampling for all the calculation models. Transition state (TS) searching was implemented using CI-NEB method.

## 2. Results and Discussion

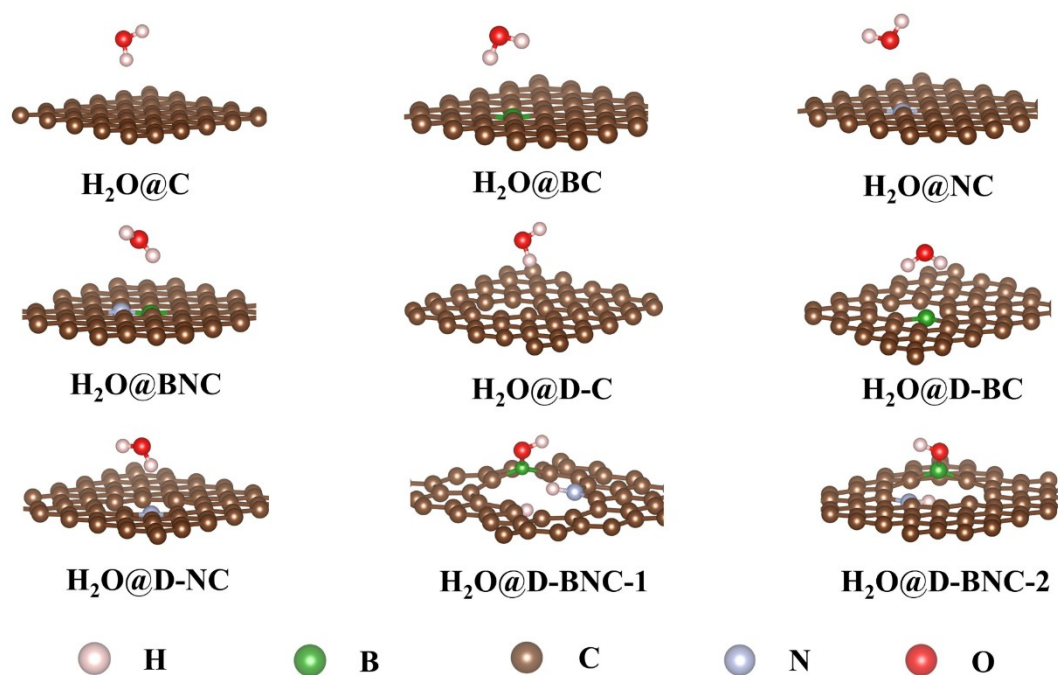


**Fig. S1.** Optimized structures of  $\text{H}_2\text{O}$  adsorption on heteroatom-doped carbon materials. C: carbon; BC: B atom doped with carbon; NC: N atom doped with carbon; BNC: B and N atoms co-doped with carbon; D-C: carbon defect; D-BC: B atom doped with a carbon defect; D-NC: N atom doped with a defected carbon; D-BNC-1: B and N (Pyrrolic N) atoms co-doped with a defected carbon; D-BNC-2 (Pyridinic N): B and N atoms co-doped defected carbon. The color codes are: H pink; B green; C brown; N blue; O red.

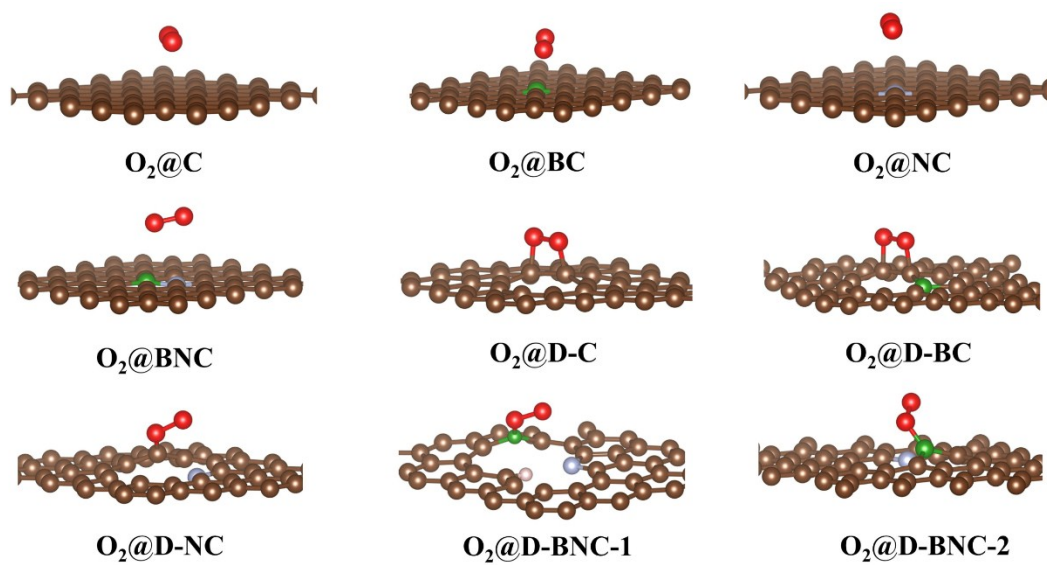


**Fig. S2.** Optimized structures of  $O_2$  adsorption on heteroatom-doped carbon materials.

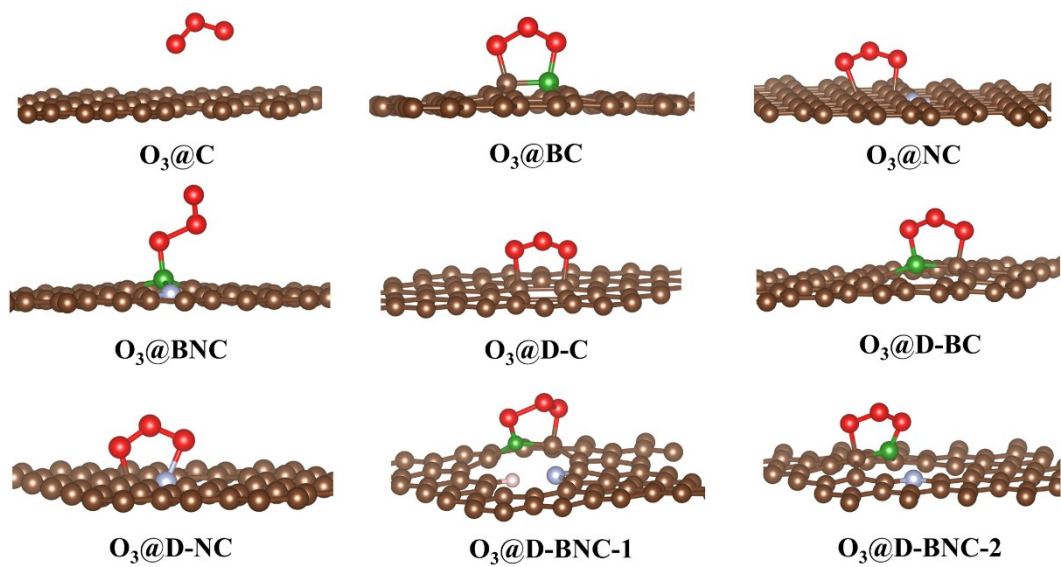


**Fig. S3.** Optimized structures of  $O_3$  adsorption on heteroatom-doped carbon materials.



**Table S1.** Summary of the heteroatom-doping concentration for different catalysts with Elemental analysis (EA) and ICP-MS.

<b>Samples</b>	<b>C (wt %)</b>	<b>N (wt %)</b>	<b>H (wt %)</b>	<b>O (wt %)</b>	<b>B (wt %)</b>
D-BNC	90.39	1.83	1.00	3.69	3.08
D-BC	91.78	0	1.00	3.49	3.28
D-NC	92.97	2.06	0.95	3.22	0
D-C	95.52	0	1.21	1.90	0
BNC	88.90	2.12	1.44	3.27	3.51

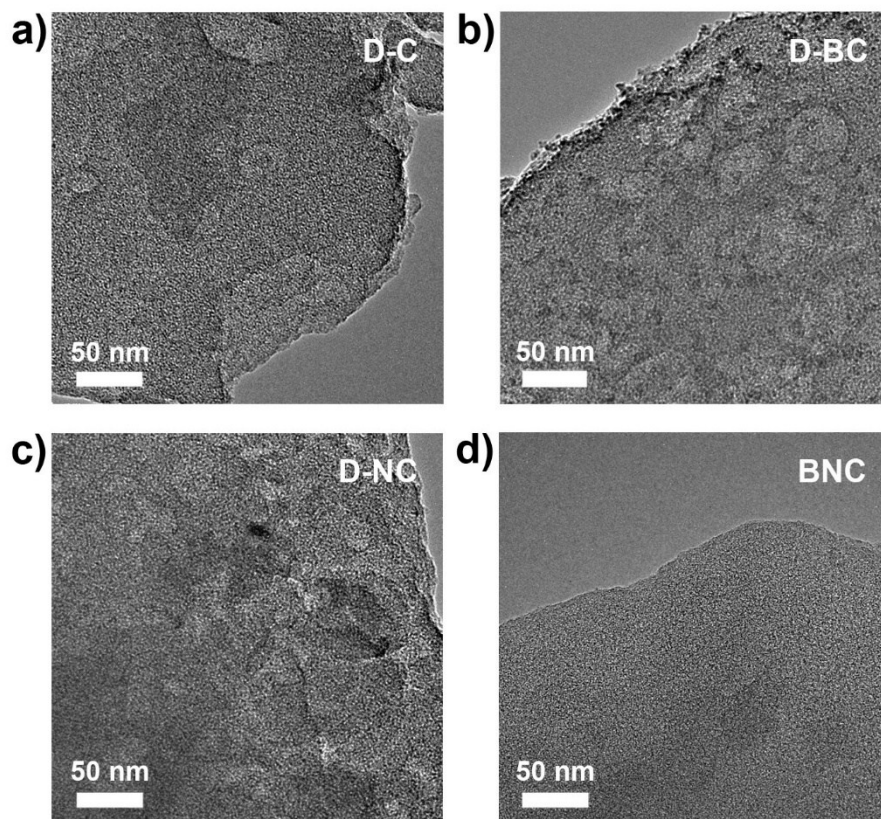


**Fig. S4.** TEM images of a) D-C, b) D-BC, c) D-NC and d) BNC.

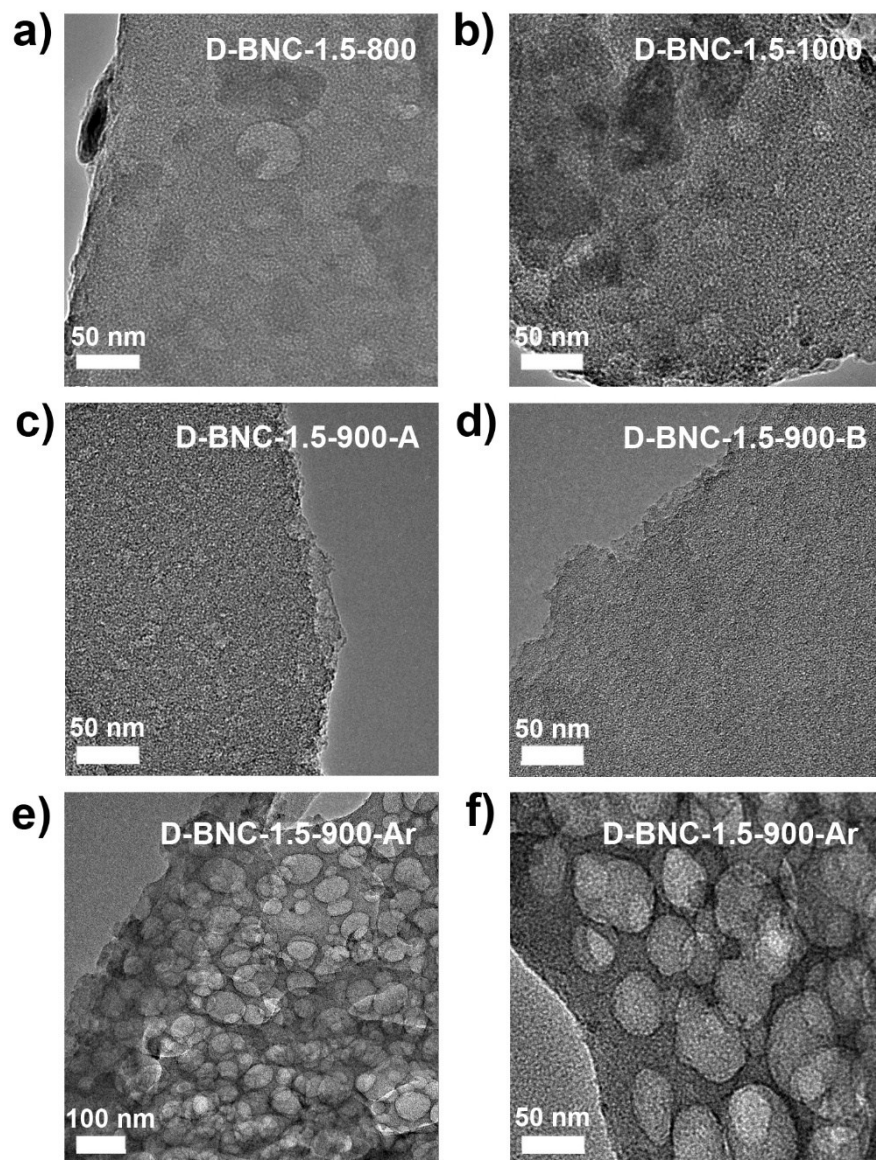


**Fig. S5.** TEM images of a) D-BNC-1.5-800, b) D-BNC-1.5-1000, c) D-BNC-1.5-900-A, d) D-BNC-1.5-900-B, e) and f) D-BNC-1.5-900-Ar.

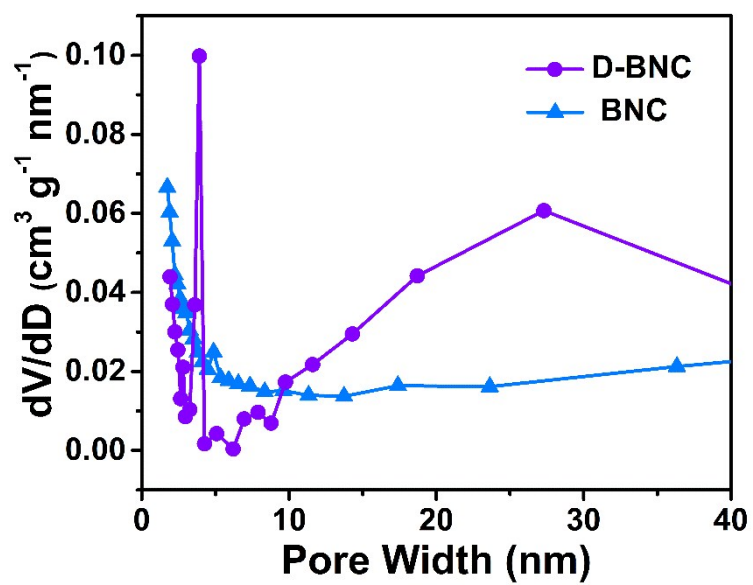


Fig. S6. The pore size distribution of D-BNC and BNC.

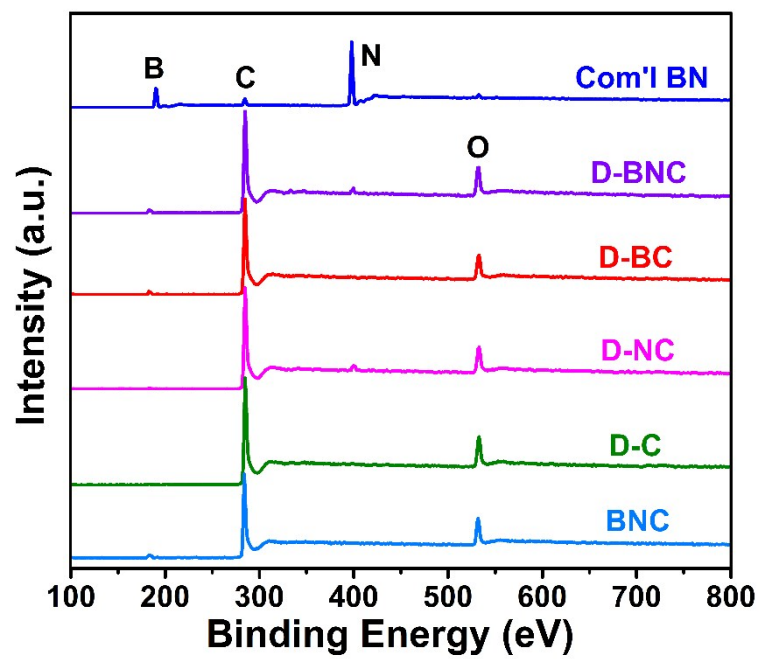
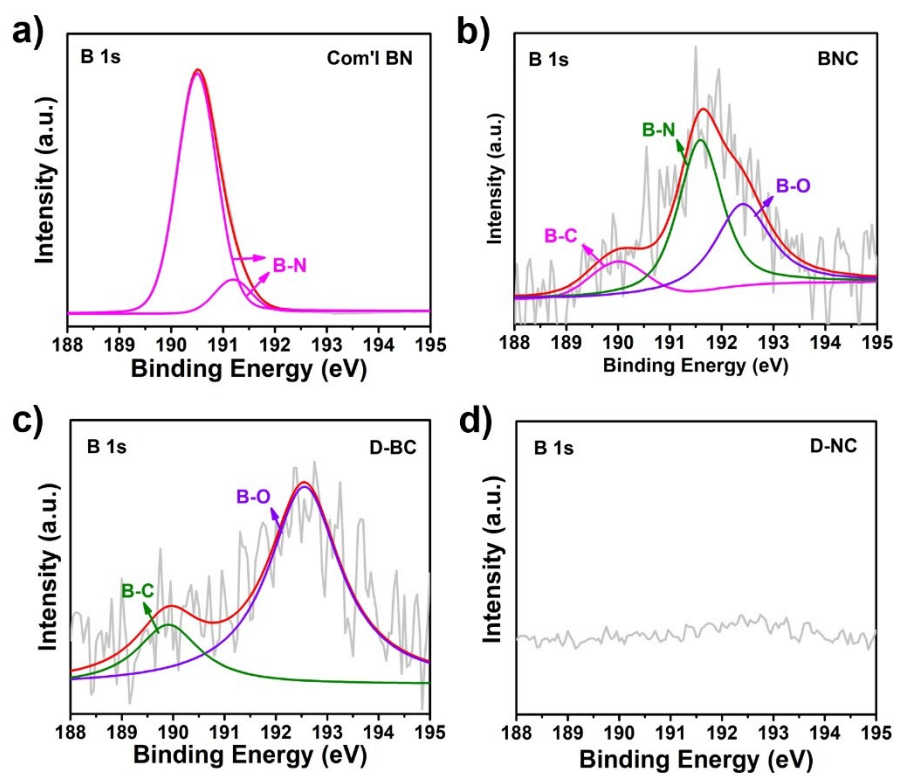


Fig. S7. XPS overall spectra of different catalysts.



**Fig. S8.** High-resolution XPS of B 1s for different catalysts.

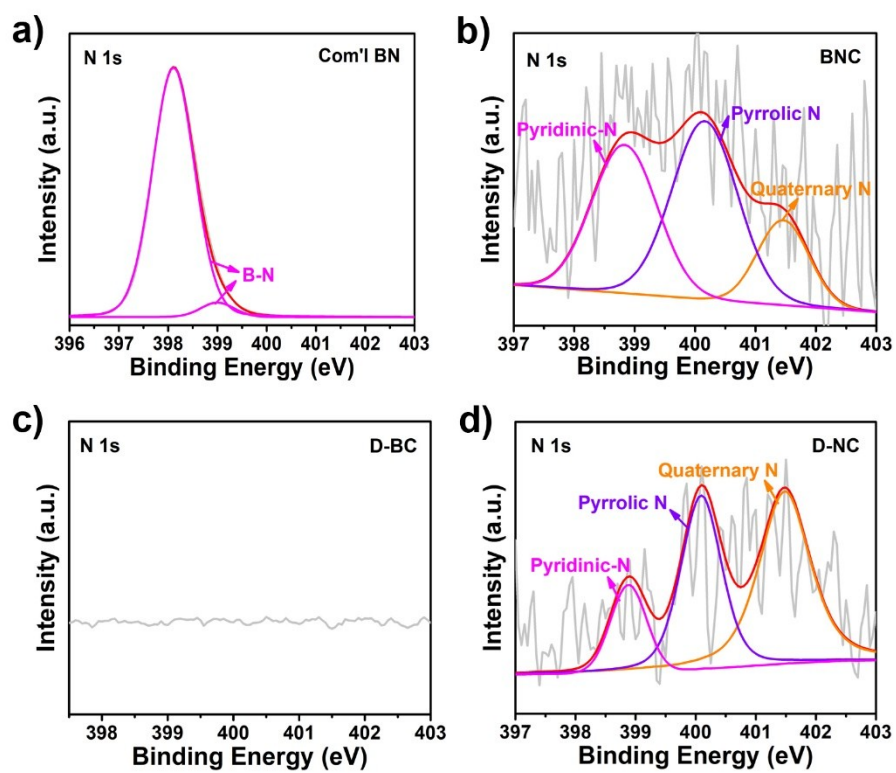
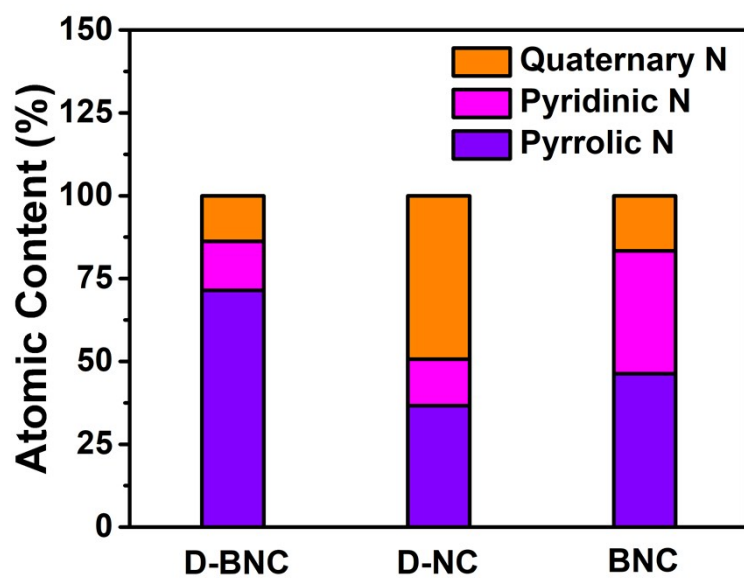


Fig. S9. High-resolution XPS of N 1s for different catalysts.



**Fig. S10.** Relative ratios of the deconvoluted peak areas of the N 1s XPS spectra.



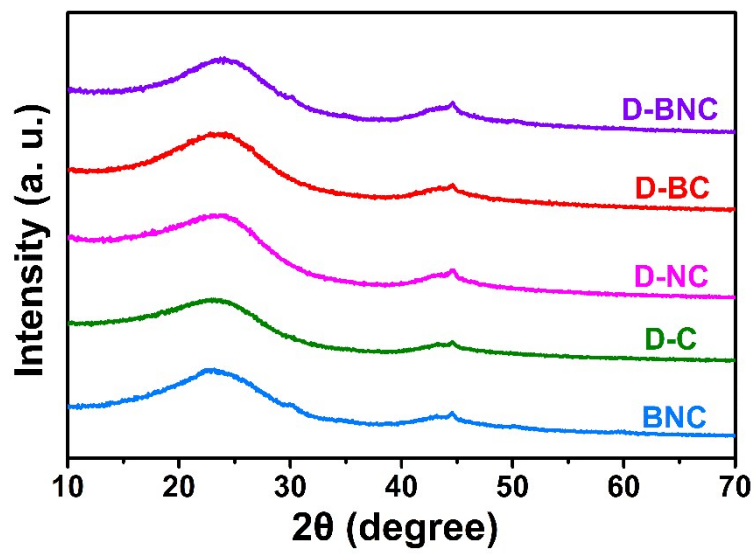


Fig. S11. XRD patterns of different catalysts.

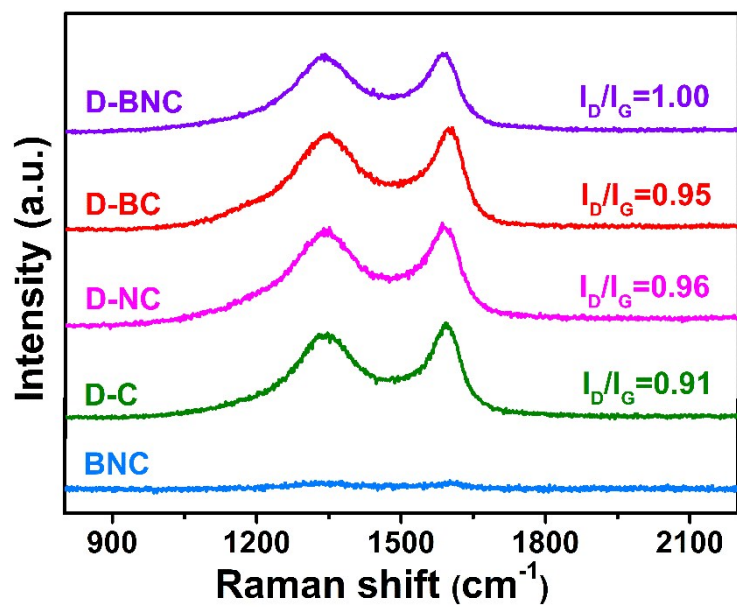
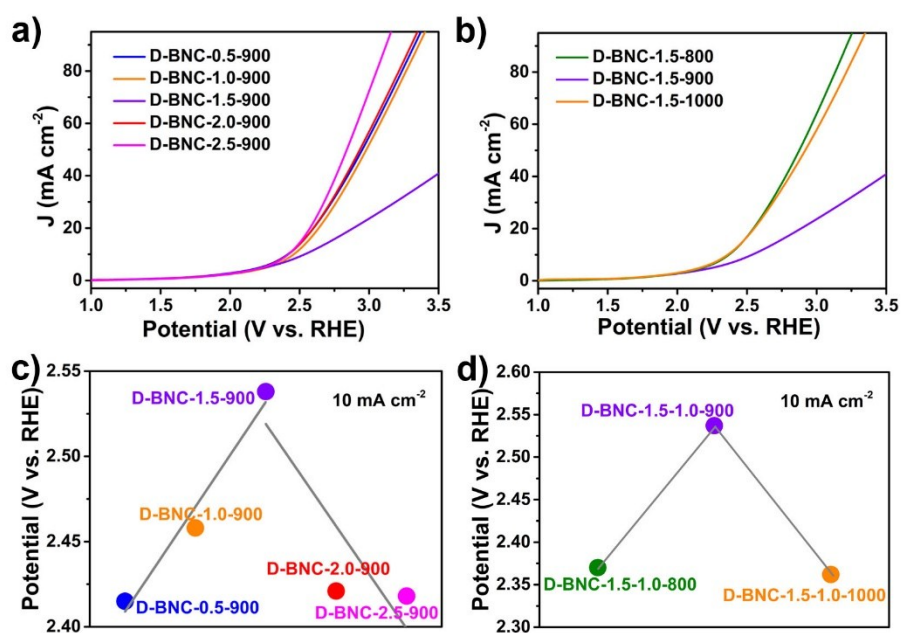


Fig. S12. Raman spectra of different catalysts.



**Fig. S13.** a, b) LSV of different catalysts electrodes obtained in the saturated potassium sulfate aqueous solution. Potential scan rate: 5 mV s<sup>-1</sup>. c, d) EOP potential of all catalysts obtained from Fig. S13a and S13b determined at a given current density of 10 mA cm<sup>-2</sup>.

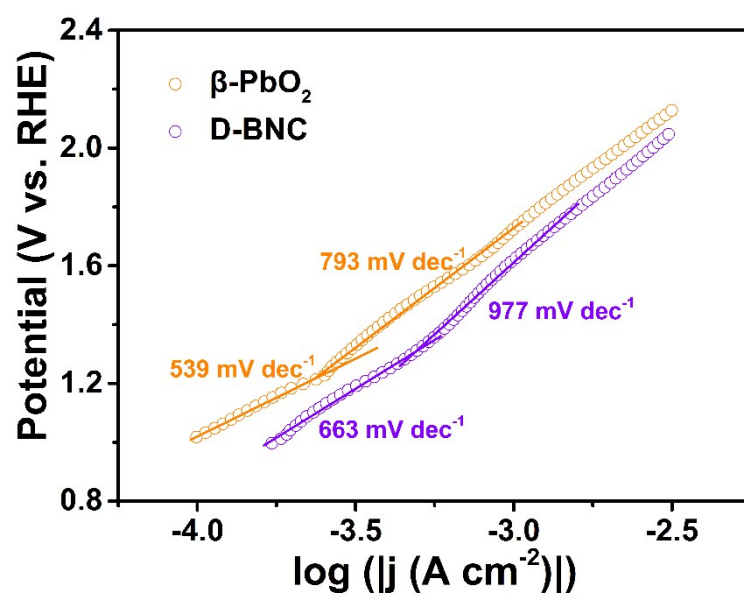
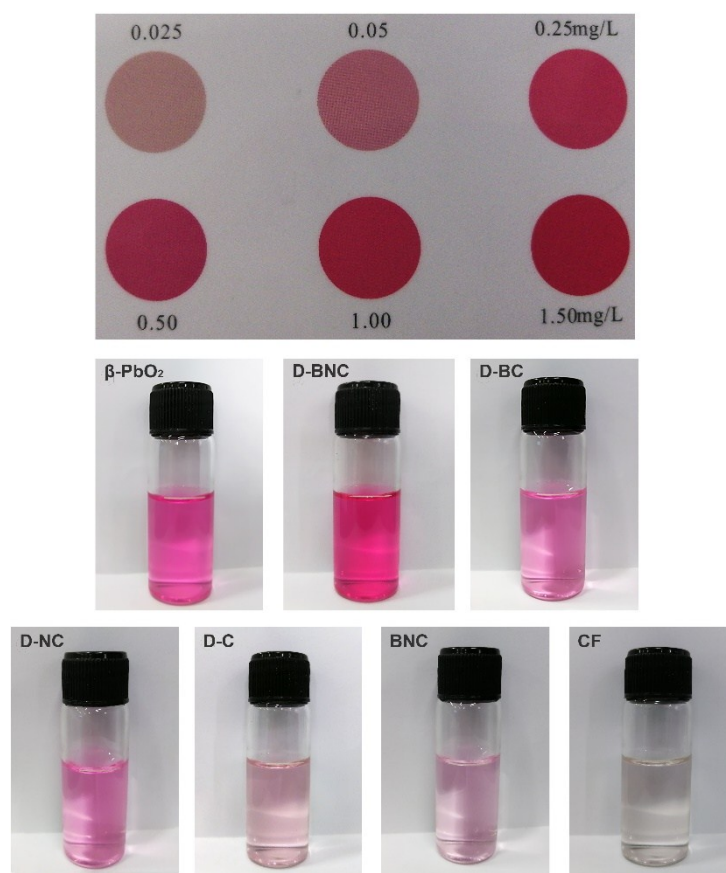
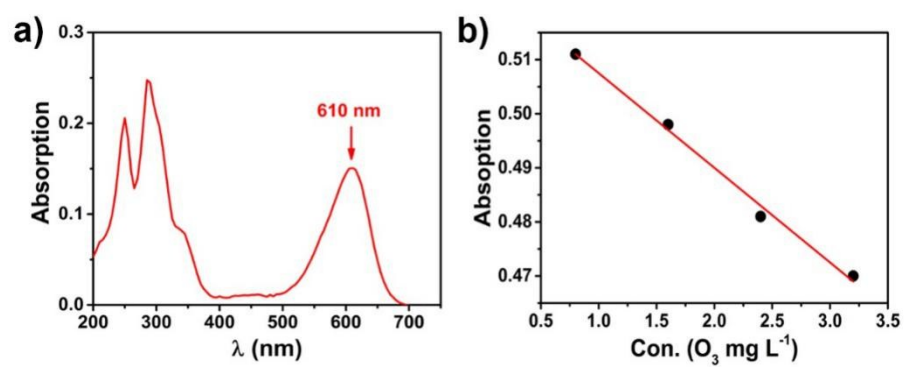


Fig. S14. Comparison between the Tafel plots of  $\beta$ -PbO<sub>2</sub> and D-BNC.



**Fig. S15.** Qualitative concentration test of dissolved ozone for different catalysts, the dissolved ozone concentrations represented by the color depth.



**Fig. S16.** a) The UV-spectra of indigo carmine solution. b) The standard curve of dissolved  $O_3$  concentration ( $y=0.525-0.0175x$ ,  $R: 0.991$ ).

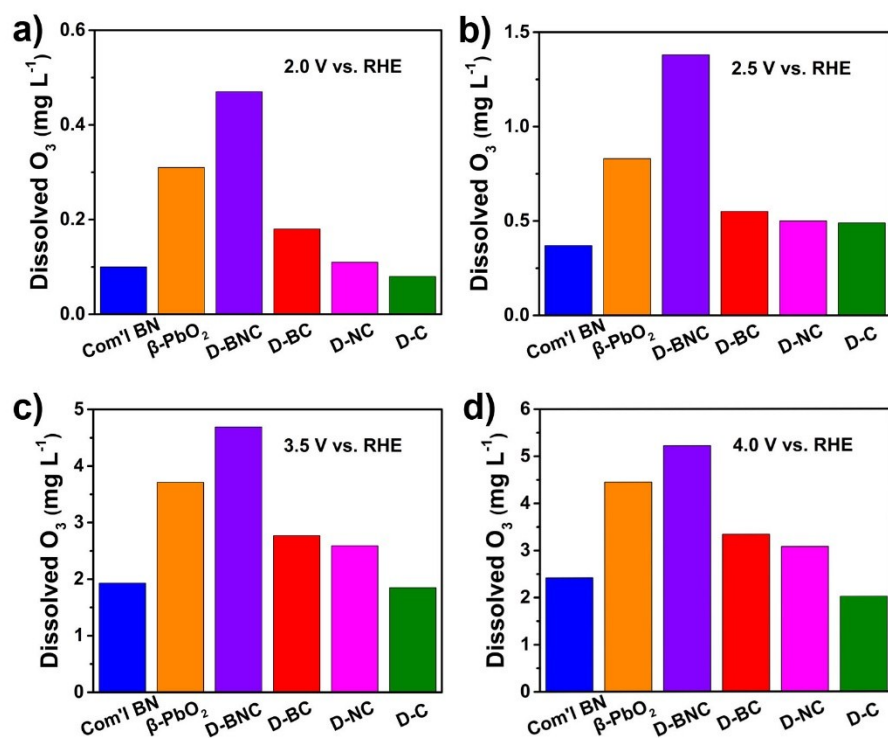


**Fig. S17.** Dissolved ozone concentrations between the different catalysts at different potential.

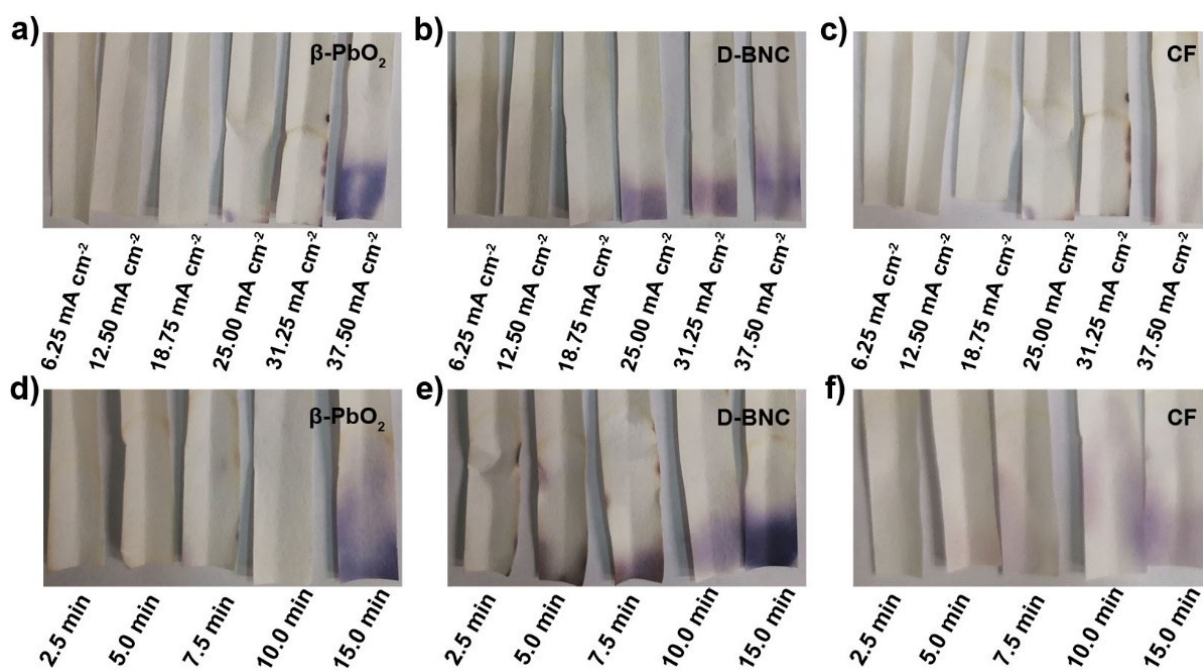


**Fig. S18.** Moistened starch potassium iodide paper giving a qualitative comparison of  $\beta$ -PbO<sub>2</sub>, D-BNC and CF a-c) with different current for 5 min and d-f) constant current test based on 25 mA cm<sup>-2</sup> for different times.



**Table S2.** The performance comparison of D-BNC with many other metal based electrocatalysts toward for EOP.

Catalysts	Electrolyte	Temperatur e	FE (%)	Ref.
<b>D-BNC</b>	<b>Neutral media</b>	<b>25 °C</b>	<b>1.7</b>	<b>This work</b>
Pt	Neutral media	20 °C	20	<i>J. Electrochem. Soc.</i> , 2009, <b>156</b> , E125-E131
Pt-TaO <sub>y</sub>	Neutral media	25 °C	19.3	<i>J. Energy Chem.</i> , 2015, <b>24</b> , 178-184
PbO <sub>2</sub>	Neutral media	30 °C	13	<i>J. Appl. Electrochem.</i> , 2010, <b>40</b> , 855-864
OFM-Fe-PbO <sub>2</sub>	Neutral media	24 °C	10	<i>J. Environ. Chem. Eng.</i> , 2016, <b>4</b> , 418-427
Ti/[TrO <sub>2</sub> -Nb <sub>2</sub> O <sub>5</sub> ]	Neutral media	0 °C	12	<i>Electrochim. Acta</i> , 2004, <b>49</b> , 1925-1935
Ni-Sb-SnO <sub>2</sub>	Neutral media	25 °C	15	<i>Green Chem.</i> , 2006, <b>8</b> , 568-572

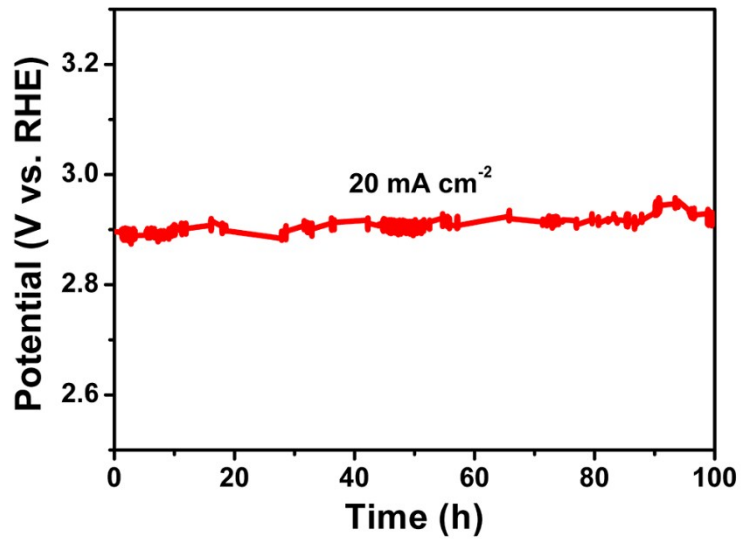


**Fig. S19.** Stability performance of D-BNC under 20 mA cm<sup>-2</sup>.

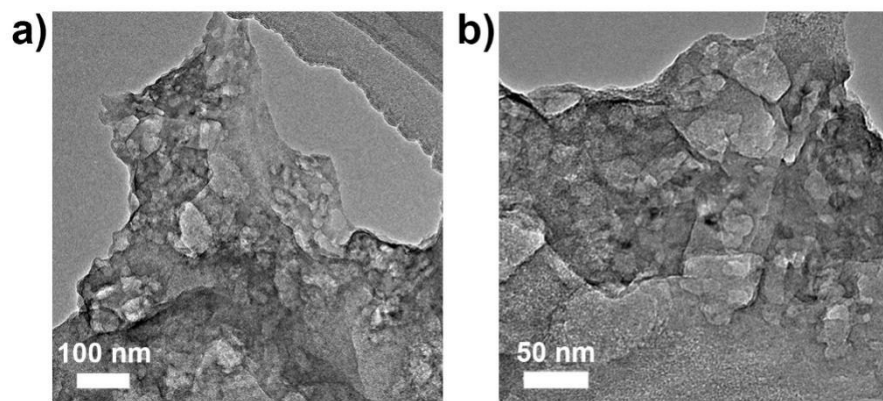


**Fig. S20.** TEM images of D-BNC after the stability evaluation.

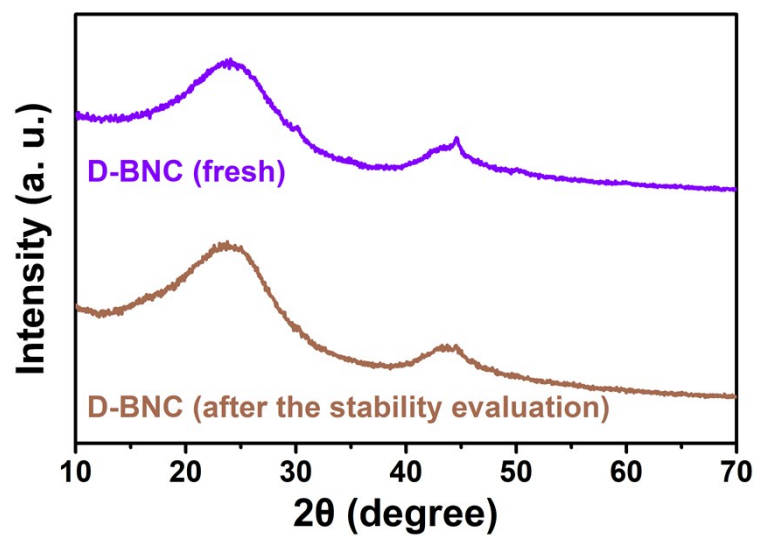


**Fig. S21.** XRD patterns of D-BNC (fresh) and D-BNC (after the stability evaluation).

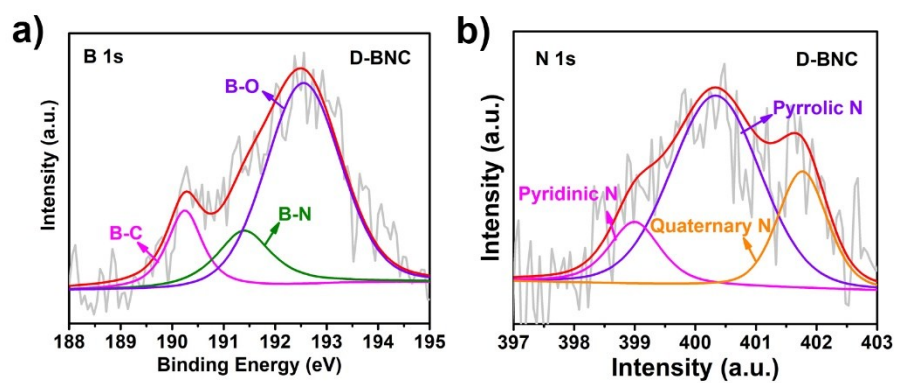


**Fig. S22.** High-resolution XPS of B 1s and N 1s for D-BNC after the stability evaluation.

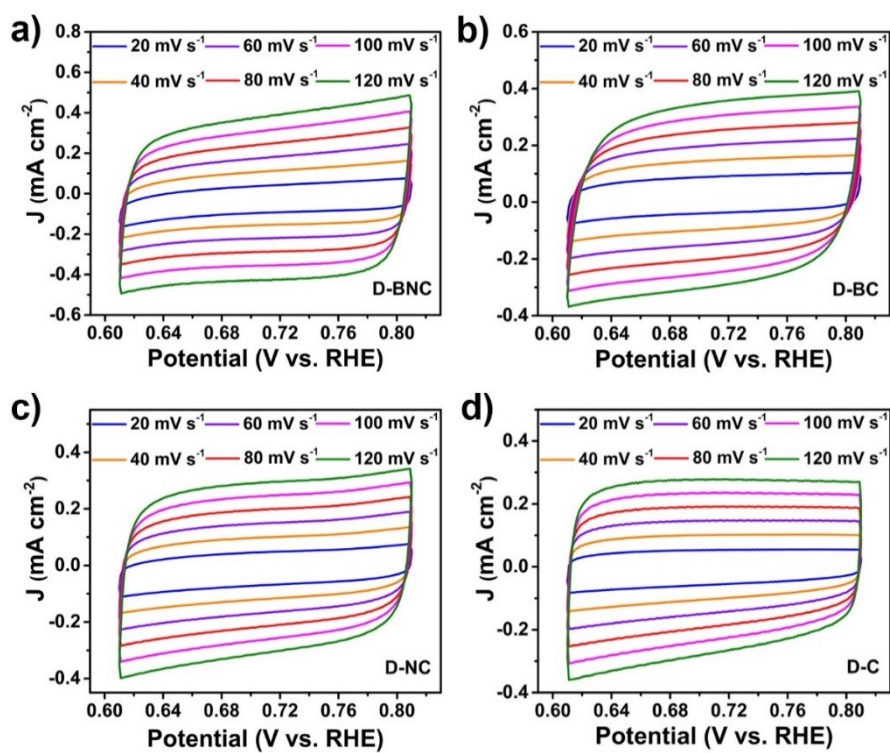


**Fig. S23.** Cyclic voltammetry curves and different scan rates to measure capacitive currents of different catalysts.

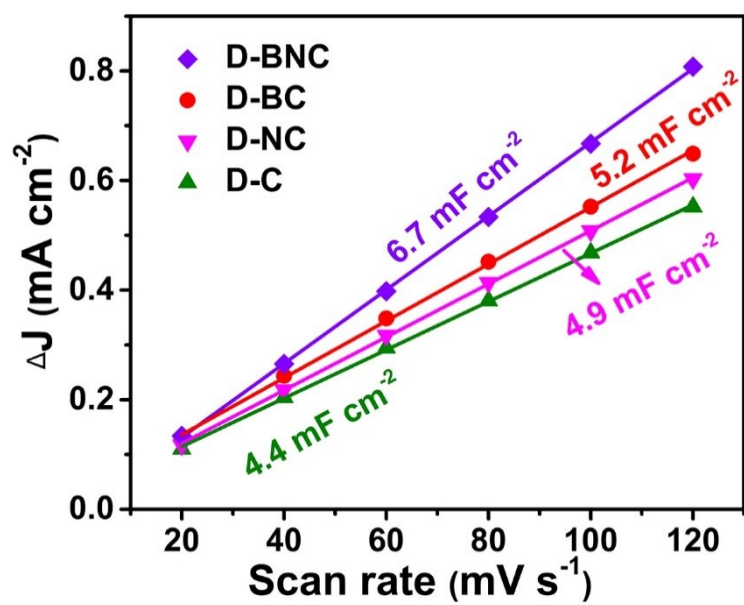


**Fig. S24.** Charging current density at  $-0.71 \text{ V}$  vs. RHE as a function of various scan rates for different catalysts.

**Table S3.** Comparison of EOP performance for D-BNC materials and other EOP electrocatalysts.

<b>Samples</b>	<b>Tafel slope (mV/dec)</b>	<b><math>J_{0, \text{geometric}}</math> (<math>\mu\text{A}/\text{cm}^2</math>)</b>	<b><math>C_{\text{dl}}</math> (mF/cm<sup>2</sup>)</b>	<b>Relative surface area</b>	<b><math>J_{0, \text{normalized}}</math> (<math>\mu\text{A}/\text{cm}^2</math>)</b>
D-BNC	977	22.39	6.7	1.52	14.73
D-BC	869	12.73	5.2	1.18	10.79
D-NC	816	12.46	4.9	1.11	11.23
D-C	817	11.68	4.4	1.00	11.68



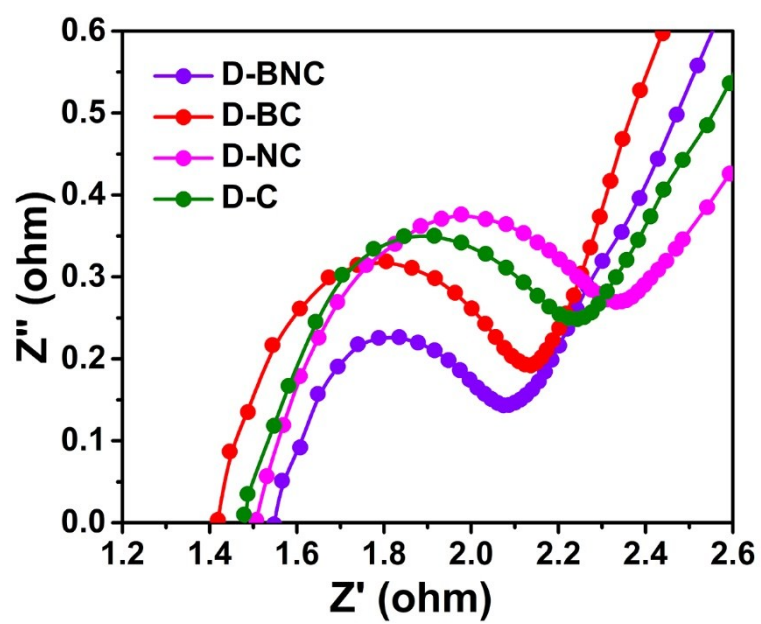
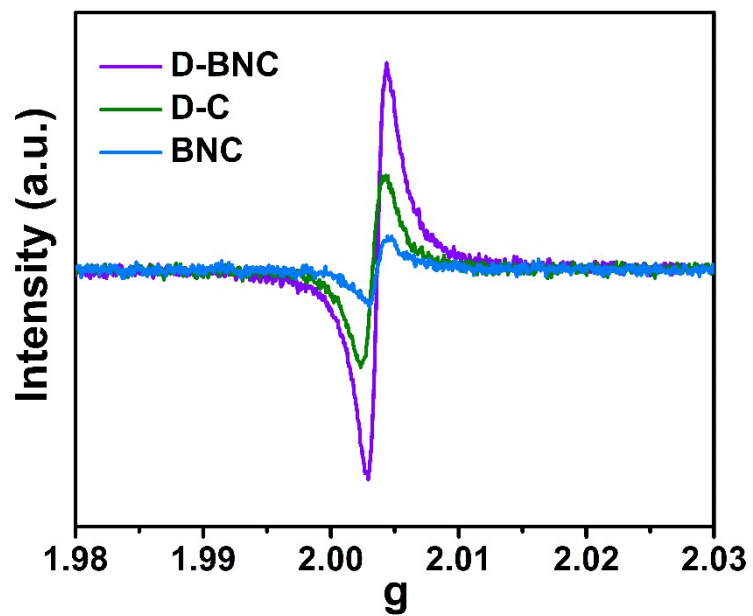


Fig. S25. Nyquist diagrams of the different catalysts.



**Fig. S26.** EPR spectrum of D-BNC D-C and BNC measured at room temperature.

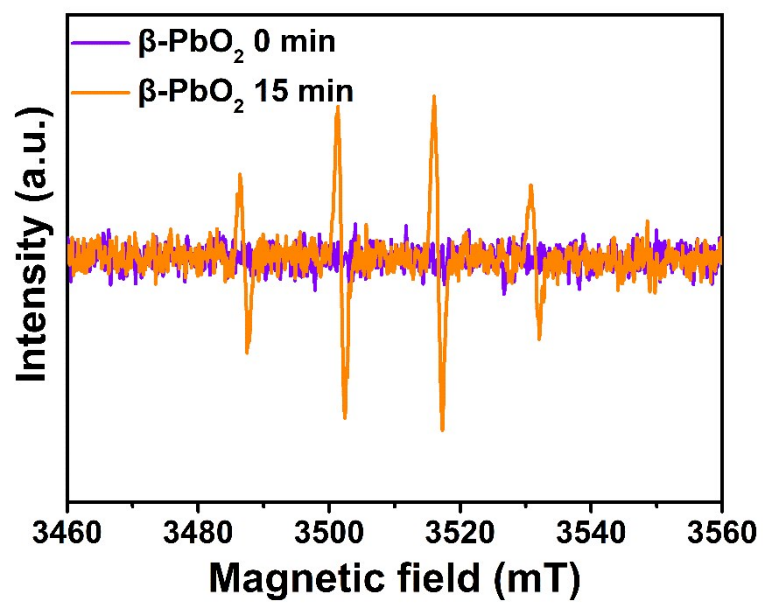
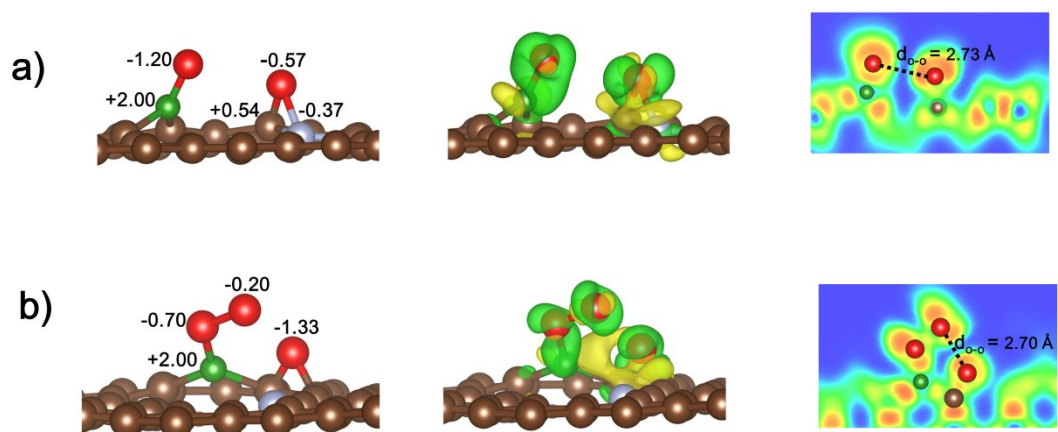
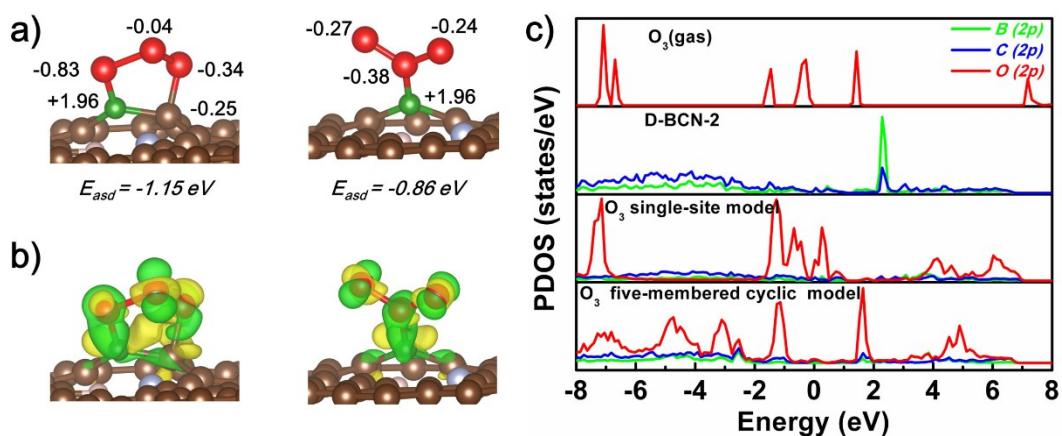


Fig. S27. ESR measurement results of DMPO-OH for  $\beta$ -PbO<sub>2</sub>.



**Fig. S28.** Optimized structures, Charge density differences (CDD) and Plots of electronic localized function (ELF) of O-O (a) and O<sub>2</sub>-O (b) intermediates adsorption on D-BNC-1.



**Fig. S29.** a) Optimized structures of O<sub>3</sub> adsorption on D-BNC for single-site and double-sites configurations, respectively. b) Charge density differences (CDD) between O<sub>3</sub> and D-BNC with the isovalue of 0.005 e Å<sup>-3</sup>. c) Partial density of state (PDOS) of O<sub>3</sub> adsorption on D-BCN-1 by single-site configuration and five-membered cyclic configuration.

### 3. References

1. Y. Meng, D. Gu, F. Zhang, Y. Shi, L. Cheng, D. Feng, Z. Wu, Z. Chen, Y. Wan, A. Stein and D. Zhao, *Chem. Mater.*, 2006, **18**, 4447-4464.
2. Y. Yan, J. Wei, F. Zhang, Y. Meng, B. Tu and D. Zhao, *Microporous Mesoporous Mater.*, 2008, **113**, 305-314.
3. S. D. Razumovskii and G. E. Zaikov, *Ozone and Its Reactions With Organic Compounds*, 1984.
4. C. Zhang, Y. F. Xu, P. Lu, X. H. Zhang, F. F. Xu and J. L. Shi, *J. Am. Chem. Soc.*, 2017, **139**, 16620-16629.